frontiers | Frontiers in Earth Science

TYPE Original Research
PUBLISHED 12 January 2023
DOI 10.3389/feart.2023.1023655

OPEN ACCESS

EDITED BY
Derek Keir,
University of Southampton,
United Kingdom

REVIEWED BY
Liang Qiu,
China University of Geosciences, China
Junling Pei,
Chinese Academy of Geological Sciences (CAGS), China

*CORRESPONDENCE
Zhenhua Li,
250759492@qq.com

SPECIALTY SECTION
This article was submitted to Structural Geology and Tectonics, a section of the journal Frontiers in Earth Science

RECEIVED 20 August 2022
ACCEPTED 02 January 2023
PUBLISHED 12 January 2023

CITATION
Li Z, Chen Z, Fan Y, Yu L, Zhang S and Li X (2023), Fission-track thermochronological evidence for the Yanshanian tectonic evolution of the northern Junggar Basin, northwest China.
Front. Earth Sci. 11:1023655.
doi: 10.3389/feart.2023.1023655

Fission-track thermochronological evidence for the Yanshanian tectonic evolution of the northern Junggar Basin, northwest China

Zhenhua Li[1]*, Zhanjun Chen[1], Yuhai Fan[2], Lan Yu[1], Suya Zhang[1] and Xiangyang Li[3]

[1]Energy Engineering Department, Longdong University, Qingyang, China, [2]China Coal Technology and Engineering Group, Xi'an, China, [3]Gansu Bureau of Coalfield Geology, Qingyang, China

The Junggar Basin is a multicycle intracontinental sedimentary basin developed on the pre-Mesozoic deformed basement. For a long time, the Junggar Basin and its adjacent Altai orogeny have been a focus of debate for geologists studying the opening and closing history of the Paleozoic Asian Ocean and Cenozoic intracontinental deformation. However, there has been no detailed research on the intracontinental tectonic activities of northern Xinjiang since the Mesozoic, particularly the Yanshanian tectonic activities in the northern Junggar Basin. Fission-track (FT) dating was conducted on 15 apatite samples and eight zircon samples obtained from the northern Junggar Basin to better understand the Yanshanian tectonic evolution. The results showed that apatite FT (AFT) ages ranged from 131 to 42 Ma and zircon FT ages ranged from 205 to 132 Ma. Based on the AFT track thermal history modeling and the regional geological data, we proposed that the northern Junggar Basin underwent three tectonic thermal events during 165–161, 93–81, and 72–66 Ma. The thermal events of 165–161 Ma may indicate magmatic activity during the Yanshanian, while the 93–86 and 72–66 Ma events reflect Late Cretaceous uplift and cooling. This study has confirmed the tectonic evolution of the Yanshanian in the northern Junggar Basin from the perspective of thermochronology. It has also revealed that the Yanshanian orogeny, a regional tectonic event, may have also occurred in northwest China.

KEYWORDS

fission-track thermochronology, yanshanian, tectonic evolution, northern junggar basin, magmatism

Introduction

Junggar Basin is an important sedimentary energy basin rich in oil, gas, and coal resources in northwest China (Xiao et al., 1992; Zhao, 1992; Cai et al., 2000). This basin is sandwiched between the Altay and Tianshan Mountains and is part of the Central Asian Orogenic Belt (CAOB). Its Paleozoic tectonic evolution is mainly characterized by a continental margin collision and orogeny. In the Late Paleozoic, the Junggar Basin and its adjacent areas formed a large tectonic collage mainly comprising island arcs, microcontinental blocks, and a paleooceanic crust (Zhang et al., 2017; Xiao et al., 2020; Zhu et al., 2020). After the Mesozoic, the Junggar Basin entered a stage of intracontinental evolution, and the tectonic activity of this basin was mainly controlled by the far-field effects of the Indian–Eurasian plate collision (Allen et al., 1994; Jolivet et al., 2001; Zhang et al., 2017). The tectonic thermal evolution and intracontinental deformation of the Junggar Basin and its adjacent areas since the

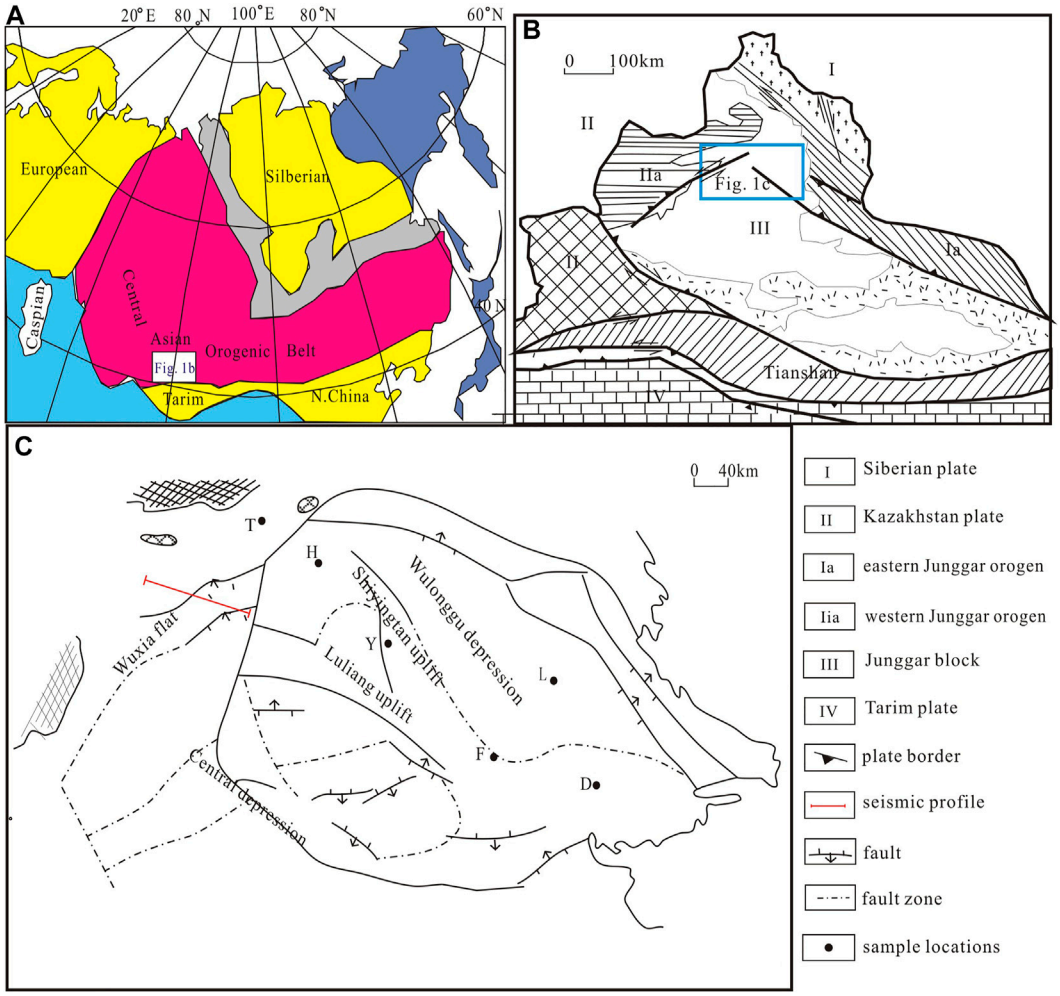

FIGURE 1
(A) Simplified tectonic map of the Central Asian Orogenic Belt. **(B)** Structural map of Junggar Basin and its adjacent areas (modified from Li et al., 2010). **(C)** Structural sketch and sample collection points of the study area.

Mesozoic have attracted the interests of many geologists (Zhou and Cai, 1990; Qiu et al., 2002; Jia et al., 2005; Wang and Xu, 2006; Dong et al., 2019; Cao et al., 2020; Hou et al., 2020; He et al., 2021; Wu et al., 2021; He et al., 2022a; Zhang et al., 2022).

Few studies have been conducted on Mesozoic tectonic activities in the Junggar Basin and its adjacent areas compared with those on Paleozoic and Cenozoic activities, and the tectonic processes and patterns during the Mesozoic are not clear. (Li et al., 2010; Yu et al., 2016; Wu et al., 2021; He et al., 2022b; Zhang et al., 2022). East Asia was widely affected by the Mesozoic Yanshanian orogeny, which resulted in complex intracontinental deformation, violent magmatic intrusions, and volcanic eruptions (Qiu et al., 2018; Yan and Qiu, 2020). This further led to substantial changes in the surface structures, landforms, paleoenvironments, and paleoecosystems of East Asia, and it is of considerable importance to the tectonics of eastern China (Dong et al., 2000; Dong et al., 2007; Dong et al., 2015; Dong et al., 2019; Faure et al., 2012; Zhu et al., 2020; Qiu et al., 2022a). Owing to the weak influence of the Yanshanian orogeny in northwest China, particularly the Junggar Basin, the Yanshanian tectonic event has not attracted considerable attention (Qiu et al., 2022b). With studies being conducted on the Yanshanian orogeny and its thermal effects in western China, researchers have gradually realized the significance of the Yanshanian orogeny for understanding mineralization in the Junggar Basin and Yanshanian tectonic evolution (Zhang et al., 1994; Dong et al., 2000; Fang et al., 2006; Guo et al., 2006; He and Gao, 2008; Yang et al., 2015; Yang et al., 2017; Sun et al., 2018; Dong et al., 2019; Zhu et al., 2020). However, the strength and timing of the Yanshanian tectonic evolution in the northern Junggar Basin are still poorly understood. Therefore, this paper will discuss the Yanshanian tectonic evolution of the northern Junggar Basin in the late Mesozoic from the tectonic thermochronology perspective.

Fission-track (FT) thermochronology was developed on the basis of the closure temperature theory and the concept of cooling age, which effectively records tectonic events in the low-temperature range and recovers corresponding geothermal histories (Gleadow et al., 1986; Gallagher et al., 1998; Ruiz et al., 2004; Ketcham et al., 2018; Tian et al., 2020a). FT thermochronology has been widely used in a variety of studies, including analysis of the thermal history of sedimentary basins, rock uplift rates, constrained stratigraphy ages, and the tectonic evolution of basins (Zhu et al., 2005; Patel et al., 2014; 2015; Ge et al., 2016; Ansberque et al., 2018; Jian et al., 2018; Bernet, 2019; Zattin and Wang, 2019; Peng et al., 2020; Tian et al., 2020b; He

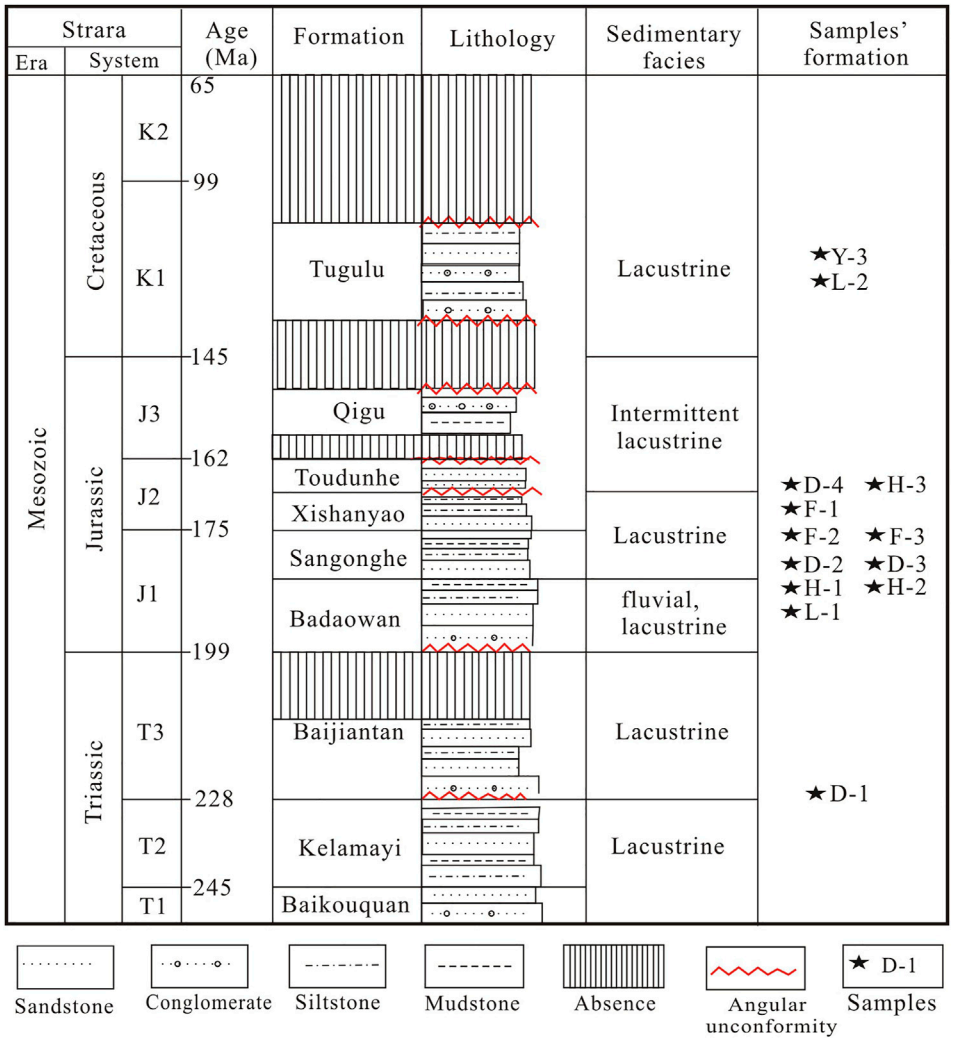

FIGURE 2
Generalized stratigraphic column of the Northern Junggar Basin showing sample locations, lithology and depositional facies.

et al., 2021; He et al., 2022a; He et al., 2022b). We studied the tectonic thermal evolution, including the peak age, of the northern Junggar Basin during the Yanshanian *via* zircon and apatite FT (AFT) dating. We concluded that the northern Junggar Basin experienced magmatism 165–161 Ma and later multiple uplift and denudation events 93–81 Ma and 72–66 Ma, respectively, which may be the response of northwest China to the Yanshanian orogeny.

Geological setting

The Junggar Basin is located in the southwestern CAOB (Figure 1A) at the intersection of the Kazakhstan, Siberia, and Tarim plates (Figure 1B). It is superimposed on the Precambrian crystalline and Hercynian-folded, metamorphic basements (Xiao et al., 1992; Li et al., 2010). Moreover, it is slightly triangular and extends for approximately 130,000 km^2. The study area, located in the northern part of the Junggar Basin, included the structural units of the Wulonggu depression, the Luliang uplift, the Shiyingtan uplift, the Dibei uplift, and the Wuxia fault-step belt. Further, it is bordered by the Zaire and Halarat Mountains to the northwest and by the Karamaili and Almantai Mountains to the northeast (Figure 1C). The evolution of the northern Junggar Basin involved five main tectonic stages: residual basin (Early Hercynian), intracontinental rift basin (Late Carboniferous to Early Permian), multicycle intracontinental compressional depression basin (Late Hercynian to Indosinian), multicycle intracontinental basin (Yanshanian to Early Himalayan), and intracontinental orogen (Mid-late Himalayan) (Zhao, 1992; Han et al., 2006; Zhang et al., 2017).

The Paleozoic in the study area is dominated by dark gray pyroclastic rocks. The Paleogene rocks are mainly purplish-red and silty mudstones with a small distribution range. Widely distributed Neogene rocks are mostly sandstones, conglomerates, and mudstones (Figure 2.). The Triassic mainly comprises gray to black mudstones interbedded with sandstones. The Early Jurassic is dominated by fluvial–lacustrine sandstones, glutenites, mudstones, and coal seams with abundant fossils. The Middle Jurassic Xishanyao Formation is dominated by fluvial–lacustrine coal-bearing clastic rocks, whereas the Toutunhe Formation is dominated by intermittent lacustrine

10.3389/feart.2023.1023655

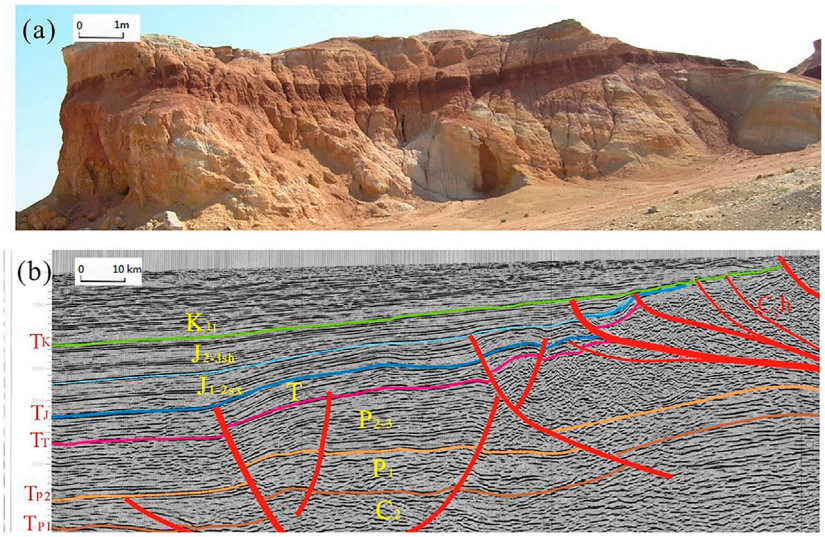

FIGURE 3
Stratigraphic unconformity in northern Junggar Basin. **(A)**The outcrop profile shows the angular unconformity between the lower Cretaceous and the upper Jurassic. **(B)** Unconformity in the study area shown by seismic profile.

TABLE 1 Details of samples used in this study.

Sample	Location	Stratigraphy	Lithology	Rock specimen
D-1	Luliang uplift	$T_{2\text{-}3xq}$	Sandstone	Drilling core
D-2	Luliang uplift	J_{1b}	Sandstone	Outcrop rock
D-3	Luliang uplift	J_{1s}	Sandstone	Outcrop rock
D-4	Luliang uplift	J_{2sh}	Sandstone	Outcrop rock
D1	Luliang uplift	C	Tuff	Drilling core
Y-1	Shiyingtan uplift	C	Tuff	Drilling core
Y-2	Shiyingtan uplift	p	Tuff	Outcrop rock
Y-3	Shiyingtan uplift	K_{1tg}	Sandstone	Outcrop rock
Y1	Shiyingtan uplift	C	Tuff	Drilling core
F-1	Luliang uplift	J_{2sh}	Sandstone	Drilling core
F-2	Luliang uplift	$J_{1\text{-}2}$	Sandstone	Outcrop rock
F-3	Luliang uplift	$J_{1\text{-}2}$	Sandstone	Outcrop rock
H-1	Shiyingtan uplift	J_{1b}	Sandstone	Outcrop rock
H-2	Shiyingtan uplift	J_{1s}	Sandstone	Outcrop rock
H-3	Shiyingtan uplift	J_{2x}	Sandstone	Outcrop rock
L-1	Wulonggu depression	J_{1s}	Sandstone	Outcrop rock
L-2	Wulonggu depression	K_{1tg}	Siltstone	Outcrop rock
T-1	Northern orogenic belt	C	Granite	Outcrop rock

brownish-red sandstones and pebbly sandstones. The Late Jurassic Qigu Formation is largely absent. The Early Cretaceous Tugulu Formation mainly comprises shallow lacustrine mudstones interbedded with sandstones, and the Late Cretaceous is mostly absent.

Based on the comprehensive analysis of outcropping rock, seismic profiles, and stratigraphic characteristics, the Yanshanian period stratigraphic unconformities in the north of the Junggar Basin are mainly between the Toutunhe and Xishanyao Formations, the Cretaceous and the Jurassic, and the Paleogene and the Cretaceous

(Figure 3). The unconformities were mostly a result of weak compression–deformation during uplift–exhumation.

Materials and methods

Samples

A total of 23 samples were analyzed, i.e., 15 samples were analyzed *via* AFT dating, and eight samples were analyzed *via* zircon fission-track (ZFT) dating. The samples were collected from surface detrital rocks from Mesozoic strata and three drill cores (wells Y, D, and F) from the study area (Table 1; Figure 1C; Figure 2). Samples D and F were obtained from Luliang uplift, among which D1 was collected from the Carboniferous drilling core, D-1 and F-1 were collected from the Triassic and Jurassic drilling cores respectively, and D-2, D-3, D-4, F-2, and F-3 were collected from the Jurassic outcrop rocks. Samples L-1 and L-2 were collected from the Jurassic and Cretaceous outcrops in the Wulonggu depression, respectively. Samples Y and H were from the Shiyingtan uplift, among which Y1 was from the Carboniferous drilling core, Y-1 was from the Jurassic drilling core, Y-2 and Y-3 were from the Jurassic and Cretaceous outcrop rocks, respectively, and H-1, H-2, H-3 were from the Jurassic outcrop rocks. Sample T-1 was collected from the Carboniferous outcrop rock on the northern edge of the Junggar Basin. The samples were mainly sandstones, siltstones, and Carboniferous to early Cretaceous tuffs. Each sample weighed more than 3 kg.

FT dating

Sedimentary detrital grains exhibit three annealing states: unreset, partial reset, and reset (Bernet and Garver, 2005; Braun et al., 2006). The FT ages of unreset grains have a low test probability (P [χ^2] < 5%) and the unreset grains are older than the stratigraphic age; this mainly represents the uplift–exhumation cooling age of a source region. Variation in the lag time between the FT age and the sedimentary age of unreset grains reveals the uplift–exhumation history of the source region. The FT ages of reset grains have a high test probability (P [χ^2] > 5%) and the reset grains are younger than the stratigraphic age; this age mainly represents the cooling age when the grains rise through the closure temperature after high-temperature annealing.

Using reset grain ages, track lengths, and thermal history modeling, we determined the tectonic thermal evolution of the Junggar sedimentary basin. The FT ages of the partial reset grains were generally older than or close to the stratigraphic age, which indicated the FT mixed ages of the partial reset grains in the source area (Braun et al., 2006). Using an appropriate statistical method to analyze these mixed ages, we can obtain the cooling age and tectonic thermal evolution information for the source region and sedimentary basin.

The closure temperature is the temperature of a thermochronological system at the time corresponding to its apparent age; it varies with grain size, chemical composition, and cooling rate (Dodson, 1973). Generally, the effective closure temperatures of apatite and zircon are approximately 120°C ± 10°C and 240°C ± 50°C, respectively (Dodson, 1973; Zaun and Wagner, 1985; Laslett et al., 1987; Hurford, 1991; Braun et al., 2006; Bernet, 2009; Tian et al., 2020a). If the grains rapidly rise through the closure temperature after high-temperature annealing, the FT age represents the cooling age of the tectonic thermal events. If the grains have been exposed to a long-term and complex thermal history after high-temperature annealing, the FT ages of the grains are mostly mixed ages, which must be analyzed and screened to obtain an effective cooling age. Commonly used methods for analyzing the FT age of a single grain include the radial chart view, P (χ^2) test, and binomial fitting. FT age groups can be directly obtained using the radial chart view method, whereby grains in the same group undergo the same thermal event. The P (χ^2) test is used to determine whether the grains belong to the same group depending on whether their ages obey the Poisson distribution. The binomial fitting method requires at least 50 grains, and their peak ages can be directly determined *via* data fitting (Galbraith and Laslett, 1993; Brandon, 1996; Brandon, 2002). Overall, the statistical distribution of FT ages, length characteristics, and peak age analyses can be used to obtain quantitative chronological constraints for tectonic thermal events.

Zircon and apatite grains used for FT analysis were separated from the samples *via* conventional heavy-liquid separation and magnetic separation techniques. FT dating was performed using the external detector method (Galbraith and Laslett, 1997) at the Institute of High Energy Physics, Beijing, China. The separated grains were mounted in epoxy resin and polyfluoroalkoxy fluororubber sheets, and the inner surfaces of the grains were exposed *via* polishing. The zircon grains were etched in a KOH–NaOH eutectic solution at 220°C for 30 h. The apatite grains were etched in a 6.6% HNO_3 solution at 25°C for 30 s to reveal the spontaneous FT. A low-uranium-content muscovite detector was used to determine induced FT density, and CN5 and CN2 uranium dosimeter glasses were used to detect apatite and zircon neutron fluxes, respectively. After irradiation, the muscovite external detector was etched in 40% HF at 25°C for 30 min, and the number of tracks was counted using a microscope (Olympus) under 1,000x magnification. The FT ages were calibrated using the zeta calibration method (Hurford and Green, 1983; Green, 1985), with a zircon zeta value of 124.1 ± 6.4 (1σ) and an apatite zeta value of 357.8 ± 6.9 (1σ).

Results

The results of the FT dating (see Tables 2, 3) showed the AFT central ages ranged from 42 ± 3 to 131 ± 9 Ma and the ZFT ages ranged from 134 ± 9 Ma to 205 ± 17 Ma; the distribution of FT ages was mainly related to tectonic units. The FT ages indicated four main age groups: 165–161, 131–122, 93–86, and 72–66 Ma. This indicates the multistage uplift–exhumation thermal evolution of the northern Junggar Basin during the Middle to Late Yanshanian.

Apatite FT dating

The P (χ^2) test is usually used to determine whether grains belong to the same group (Galbraith and Green, 1990; Galbraith and Laslett, 1993). P (χ^2) > 5% means that the grains belong to the same group and undergo a single cooling process. P (χ^2) < 5% means that the grains belong to different groups and represent a mixed age, for example, when the grains come from different source regions and remain in the partial annealing zone for a long period. The AFT dating results (Table 2; Figure 4) indicated that the P (χ^2) of all the samples was >5%, and the track length of

TABLE 2 Apatite fission track data of the northern Junggar Basin.

Sample	Grains(n)	Stratigraphyage	ρ_s (10^5/cm) (Ns)	ρ_i (10^5/cm) (Ni)	ρ_d (10^5/cm) (N)	P (χ^2) (%)	Central age (Ma) (±1σ)	Pooled age (Ma) (±1σ)	L (μm) (N)
D-1	29	$T_{2\text{-}3xq}$	2.728 (503)	4.581 (852)	8.130 (10,300)	100	93 ± 6	93 ± 6	10.9 ± 2.0 (104)
D-2	27	J_{1b}	3.192 (423)	7.248 (1,454)	97.4 (10,300)	98.1	72 ± 4	72 ± 4	11.1 ± 1.8 (101)
D-3	28	J_{1s}	4.175 (685)	8.422 (1,453)	9.582 (10,300)	91.7	92 ± 5	92 ± 5	11.6 ± 1.7 (106)
D-4	29	J_{2sh}	4.584 (542)	9.702 (1,176)	9.693 (10,300)	100	88 ± 6	88 ± 6	11.5 ± 1.6 (92)
Y-1	28	C	.877 (118)	1.226 (165)	8.911 (10,322)	100	122 ± 15	122 ± 15	10.4 ± 2.0 (105)
Y-2	28	P	2.262 (149)	2.657 (175)	7.906 (10,322)	99.9	128 ± 15	128 ± 15	12.2 ± 2.3 (103)
Y-3	28	K_{1tg}	3.702 (564)	7.029 (1,071)	8.576 (10,300)	98.2	86 ± 5	86 ± 5	11.3 ± 1.7 (104)
F-1	12	J_{2sh}	7.500 (443)	30.467 (1,687)	8.800 (10,300)	55.1	42 ± 3	42 ± 3	11.4 ± 1.6 (54)
F-2	23	$J_{1\text{-}2}$	3.656 (806)	8.685 (1932)	8.688 (10,300)	7.5	66 ± 5	70 ± 4	12.1 ± 1.9 (108)
F-3	31	$J_{1\text{-}2}$	5.308 (1,142)	12.262 (2,518)	8.130 (10,300)	59.0	67 ± 3	67 ± 3	11.8 ± 2.0 (102)
H-1	27	J_{1b}	4.350 (860)	6.298 (1,315)	9.805 (10,300)	100	129 ± 7	129 ± 7	12.3 ± 1.7 (92)
H-2	28	J_{1s}	1.094 (492)	1.472 (647)	9.247 (10,300)	100	131 ± 9	131 ± 9	13.5 ± 2.1 (115)
H-3	13	J_{2x}	2.907 (340)	7.557 (525)	8.688 (10,300)	12.5	67 ± 8	64 ± 6	12.5 ± 2.2 (40)
L-1	28	J_{1s}	4.040 (1,232)	6.887 (1890)	9.805 (10,300)	25.2	108 ± 6	110 ± 5	12.7 ± 1.8 (107)
L-2	27	K_{1tg}	3.536 (642)	6.648 (1,248)	9.917 (10,300)	71.2	101 ± 6	101 ± 6	12.8 ± 1.6 (112)

Note: n is the number of grains analyzed; ρs is spontaneous fission track density; N_S, is the number of spontaneous fission tracks counted; ρi is induced fission track density; Ni is the number of induced fission tracks counted; ρd is fission track density measured in dosimeter glass CN5; Nd is the number of induced fission tracks counted in dosimeter glass CN5; P (χ^2) is chi-square probability; σ is the error of mean confined track lengths; L is mean confined fission track length; N is the number of tracks.

TABLE 3 Zircon fission track data of the northern Junggar Basin.

Sample	Grains (n)	Stratigraphy age	ρs (10^5/cm) (Ns)	Pi (10^5/cm) (Ni)	ρd (10^5/cm) (N)	P (χ^2) (%)	Central age (Ma) (±1σ)	Pooled age (Ma) (±1σ)
D-1	21	$T_{2\text{-}3xq}$	108.264 (2,246)	18.106 (362)	3.353 (5,868)	33.1	134 ± 9	135 ± 9
D-2	20	J_{1b}	145.521 (1,649)	22.541 (264)	3.691 (5,868)	0.5	165 ± 16	165 ± 14
D1	23	C	132.233 (4,556)	19.154 (644)	3.402 (5,868)	1.3	151 ± 10	151 ± 9
Y1	22	C	135.304 (3,405)	17.451 (454)	3.476 (5,868)	24.3	174 ± 13	176 ± 12
F-3	19	$J_{1\text{-}2}$	143.861 (3,013)	24.041 (501)	3.680 (5,868)	59.1	146 ± 9	146 ± 9
H-1	25	J_{1b}	135.174 (5,036)	18.440 (684)	3.327 (5,868)	66.2	161 ± 10	161 ± 10
L-1	21	J_{1s}	143.134 (4,288)	18.694 (587)	3.252 (5,868)	38.8	163 ± 10	163 ± 10
T-1	23	C	98.461 (2,410)	11.889 (291)	3.828 (5,933)	27.6	205 ± 17	207 ± 16

Note: n is the number of grains analyzed; ρs is spontaneous fission track density; N_S, is the number of spontaneous fission tracks counted; ρi is induced fission track density; Ni is the number of induced fission tracks counted; ρd is fission track density measured in dosimeter glass CN2; Nd is the number of induced fission tracks counted in dosimeter glass CN2; P (χ^2) is chi-square probability; σ is the error of mean confined track lengths.

10.3389/feart.2023.1023655

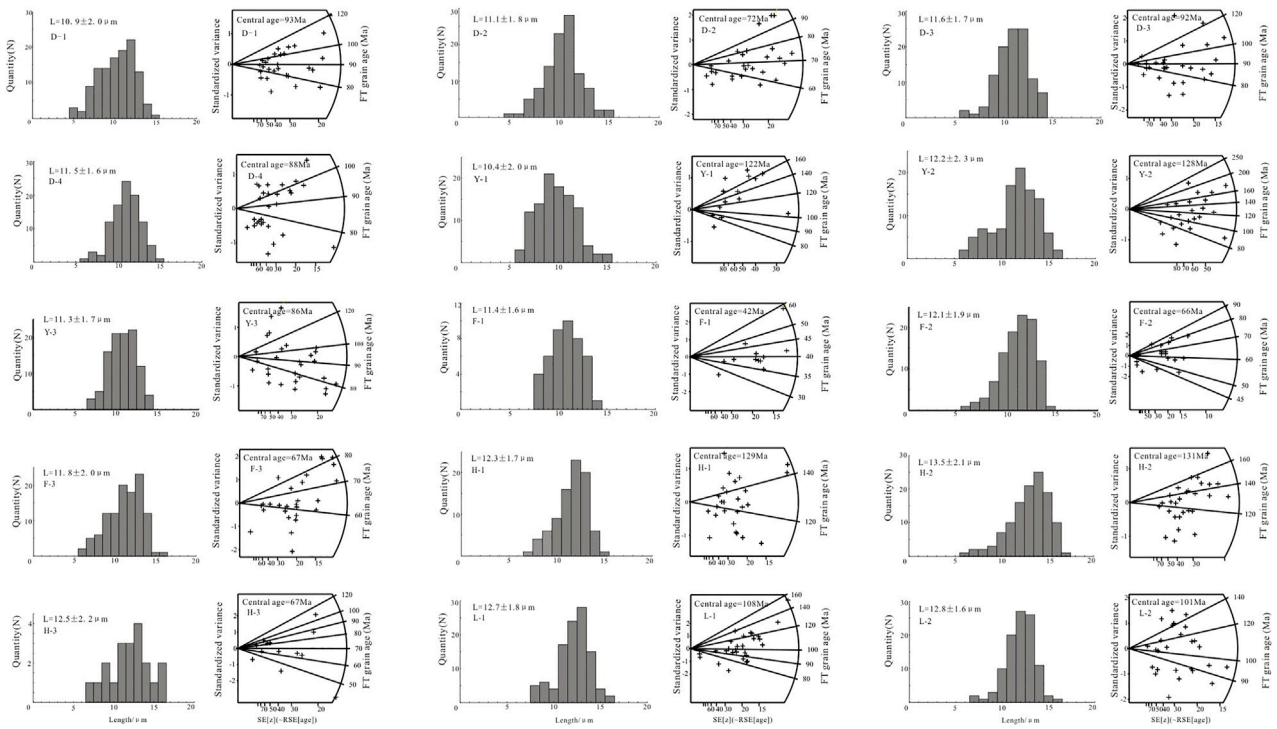

FIGURE 4
Fission track length histograms and radiograms of apatite grains from the northern Junggar Basin. The left panels of each group are fission track length histograms, the right panels are fission track radiograms, in which, *X* and *Y*-axes represent the age accuracy and standard deviations of single grains, respectively.

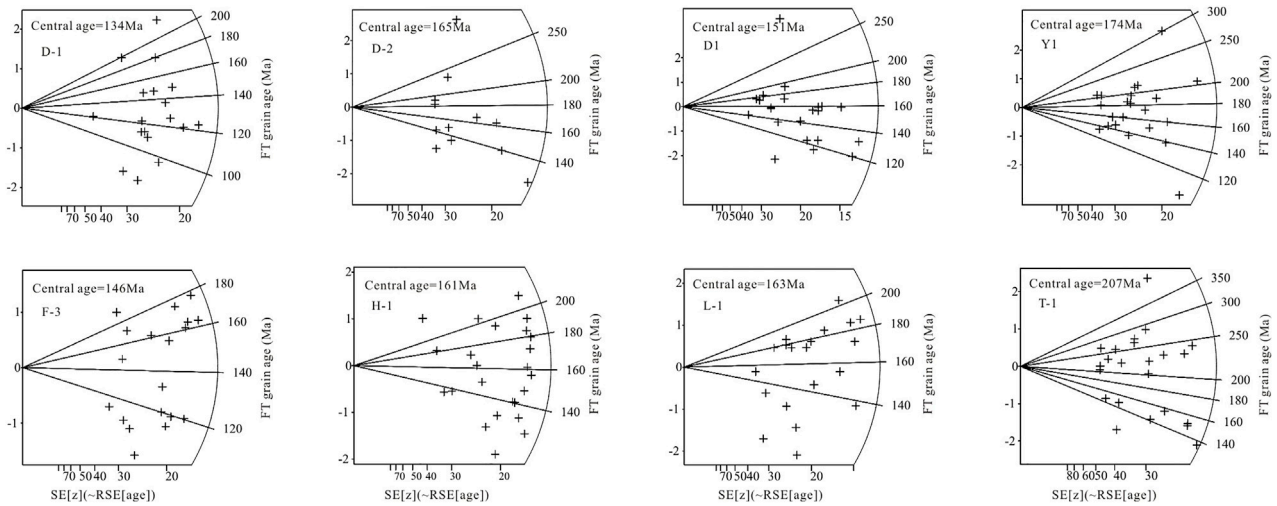

FIGURE 5
Radiograms of ZFT single grain ages from the northern Junggar Basin. *X* and *Y*-axes represent the age accuracy and standard deviations of single grains, respectively.

the grains presented a single peak. This indicated that the sampled grains belong to a single age group, which means that all the sampled grains underwent a single cooling process. The AFT central ages ranged from 42 ± 3 to 131 ± 9 Ma, and the peak ages were mainly 131–122, 93–86, and 72–66 Ma.

Zircon FT dating

The ZFT dating results are shown in Table 3 and Figure 5. Six samples showed P (χ^2) > 5%, indicating that the grains belong to the same group. The D-2 and D1 samples showed P (χ^2) < 5%, indicating

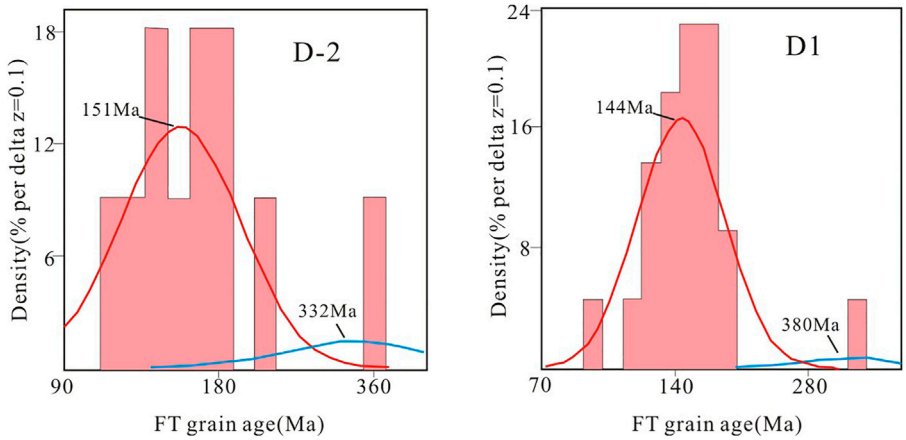

FIGURE 6
Frequency histograms of single grains of ZFT ages and age components calculated by binomial fitting method.

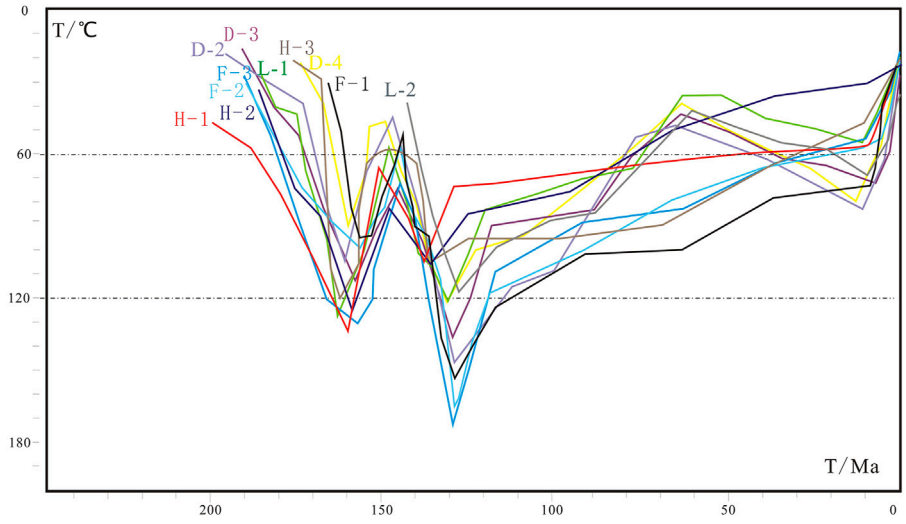

FIGURE 7
Results of thermal history modeling.

mixed ages. These two samples were analyzed using the binomial fitting method (Figure 6). Sample D-2 had peak ages of 144 and 380 Ma, and sample D1 had peak ages of 151 and 332 Ma. Because the ages of 380 and 332 Ma were older than the stratigraphic age of the samples, they reflected the thermal history of the grains in the source regions. Therefore, we determined the peak ages to be 144 and 151 Ma, representing the thermal history of the basin. Overall, the ZFT ages ranged from 134 ± 9 Ma to 205 ± 17 Ma, and the peak ages were mainly 165–161 Ma.

Thermal history modeling

Shortening AFT patterns reflect cooling paths through the apatite partial annealing zone. Important information can be obtained by modeling the thermal history of apatite grains using specific ages and track lengths, including the timings and temperatures of tectonic thermal events in basins. The partial annealing zone is defined as the temperature range in which FTs can be partially retained on a geological time scale. The track will be completely annealed when the temperature is above that zone, and it will be well preserved when the temperature is below that zone. When the temperature is within this range, the FT length will shorten or become non-existent, and a new fission track will be simultaneously produced. Generally, the partial annealing zone of apatite is 60°C–120 °C (Braun et al., 2006; Tian et al., 2020a).

In this study, the AFTSolve program (Ketcham, 2005) was used to model the time–temperature path based on the grain ages and track lengths of 11 typical samples. The initial Dpar value was 1.5 μm, and the initial track length was calculated based on the Dpar value. The initial modeling temperature is the temperature of the stratum during deposition, generally approximately 20°C; therefore, it was set as

10°C–30°C. The maximum burial time and temperature range were the modeling constraints, and the modeling temperature was less than the maximum burial temperature of the stratum. For each sample, inverse thermal history modeling was run for 100,000 paths to find the best fitting curve. The modeling results (Figure 7) showed that there were two tectonic thermal events in the northern Junggar Basin during the Yanshanian, which resulted in partial or complete annealing of apatite. The first tectonic thermal event (buried heating) occurred between 165 and 161 Ma, and the second tectonic thermal event occurred between 131 and 128 Ma.

Discussion

Yanshanian magmatism

Large-scale magmatic activities mainly occurred in the Junggar Basin and its adjacent areas during the Paleozoic. The intracontinental tectonic thermal evolution started in the Mesozoic (Xiao et al., 1992; Qiu et al., 2002); therefore, magmatic activities were substantially weakened, resulting in reduced volcanic age records. However, based on detrital zircon geochronology, large numbers of late Mesozoic magmatism have been recorded for detrital materials collected from the Junggar Basin. For example, *via* zircon U–Pb dating, Yang et al. (2013) obtained peak ages of 144 and 162 Ma from the Manas section of the Junggar Basin, Fang et al. (2015) obtained a peak age of 153 Ma for the grains obtained from the Toutunhe section, and Zhu et al. (2020) obtained peak ages of 132 and 169 Ma for the grains obtained from the Wangjiagou section and 161 Ma for the grains obtained from the Kelamaili section. Additionally, Liu et al. (2018) used laser ablation inductively coupled plasma mass spectrometry to obtain a zircon U–Pb age of 189 Ma for the grains obtained from the northeastern Junggar Basin, confirming the existence of Early Jurassic magmatism in the northeastern Junggar Basin.

Yanshanian magmatism in orogenic belts adjacent to the Junggar Basin has also been studied, particularly in the Altay and Tianshan areas. Zhang et al. (1994) determined a tectonomagmatic Ar–Ar age of 131 Ma (Middle Yanshanian) for granites in the Altay area. Chen et al. (1999) obtained an Ar–Ar age of 149–135 Ma from tectonic thermochronological records for granites in the Altay area. Zircon U–Pb ages of 154.9 ± 1.9 Ma and 152.7 ± 1.8 Ma were determined for Eastern Tianshan by Liu et al. (2019). These studies have confirmed the existence of Yanshanian magmatism around the Junggar Basin.

In our study, ZFT ages ranged from 205 to 132 Ma, with a peak age of 165–161 Ma. Except for samples D-1 and T-1, the FT ages of other samples were concentrated at approximately 160 Ma, indicating that the study area experienced important tectonic thermal events during this period. Generally, the FT age of the old strata in the same area should be newer than that of the new strata above it. However, the Carboniferous sample T-1 has the oldest FT age of 205 ± 17 Ma. This may be related to the fact that the sample was collected from the orogenic belt on the northern margin of the Junggar basin, which has experienced different tectonic evolution processes. High temperatures are required for annealing and partial annealing of zircon owing to its high closure temperature (240 °C ± 50 °C). Considering the evidence of the existence of Middle Yanshanian magmatism in the Junggar Basin and the two tectonic thermal events that resulted in the partial or complete annealing of apatite, we chose to interpret the tectonic thermal event that occurred from 165 to 161 Ma to be a result of magmatism. The AFT ages ranged from 131 to 42 Ma, with peak ages of 131–122 Ma, 93–86 Ma, and 72–66 Ma. The FT ages of the four samples, Y-1, Y-2, H-1, and H-2, were distributed between 122 and 131 Ma. These samples were collected from the Shiyingtan uplift, and the sampling points were relatively close, which may reflect a tectonic thermal event of 130 Ma. Considering that the closure temperature of zircon is higher than that of apatite, the ZFT (165–161 Ma) and AFT ages (131–122 Ma) probably represent FT age recordings of the same tectonic thermal event, possibly reflecting a nearly continuous Yanshanian tectonic thermal event.

Yanshanian tectonic events are also reflected in the sedimentary characteristics and contact relationships of the strata. The appearance of intermittent brownish-red lacustrine sandstones in the Toutunhe Formation shows that the climate tended toward an arid environment. The angular unconformity at the top of the Toutunhe Formation and the absence of the Upper Jurassic strata (Figure 3) indicate that uplift may have started after the deposition of the Toutunhe Formation in the Middle Jurassic. An unconformity at the base of the Cretaceous is widely developed across the whole region and the whole of western China. This indicates a strong tectonic event that lasted from the Middle to Late Jurassic to the Early Cretaceous. Based on the most recent international stratigraphic age of 163.5 Ma for the Upper Jurassic and our newly obtained 165–161 Ma ZFT ages, we consider the start of the Yanshanian orogeny in the northern Junggar Basin to be approximately 163 Ma.

Uplift and cooling events in the Late Yanshanian

Our new AFT ages show that there were two uplift and cooling events at 93–86 and 72–64 Ma, which correspond to the widespread absence of Upper Cretaceous strata in the study area. Additionally, these uplift and cooling events are also reflected in the sedimentary characteristics and contact relationships of adjacent areas. For example, Upper Cretaceous strata are absent in the eastern Tarim Basin, and Paleogene strata directly overlie Lower Cretaceous strata. There is an angular unconformity between Upper Cretaceous and Lower Cretaceous strata in the Turpan–Hami Basin and between Upper Cretaceous and Lower Jurassic strata in the western Tianshan Mountains (Zhu et al., 2005; 2020; He and Gao, 2008; Yang et al., 2015; 2017). Thermochronology studies have also documented Late Cretaceous uplift–exhumation events in the Junggar Basin and its adjacent areas: AFT ages of 90–25 Ma for an uplifting event in northern Junggar Basin (Li et al., 2010; Li et al., 2014); AFT ages of 120–45 Ma for cooling stages in the southern margin of the Junggar Basin (Zhang et al., 2022); AFT thermochronology and seismic profiles revealed a rapid uplift (ca. 100–60 Ma) in the Late Cretaceous Paleocene in the eastern Junggar Basin (Wu et al., 2021); AFT ages of 120–60 Ma for Cretaceous uplifting events in the Altai region (Yuan et al., 2004; Johan et al., 2006); AFT ages of 110–70 Ma for a rapid uplift–exhumation event in the Tianshan Mountains (Hendrix et al., 1994; Guo et al., 2002; Glorie et al., 2010; Luo et al., 2012; Zhang et al., 2017); and the Eastern Tianshan and southern part of the east Junggar experienced moderate to rapid basement cooling throughout the Cretaceous (He et al., 2022b). These studies indicate that an uplift–exhumation event occurred during the Late Cretaceous that affected the Junggar

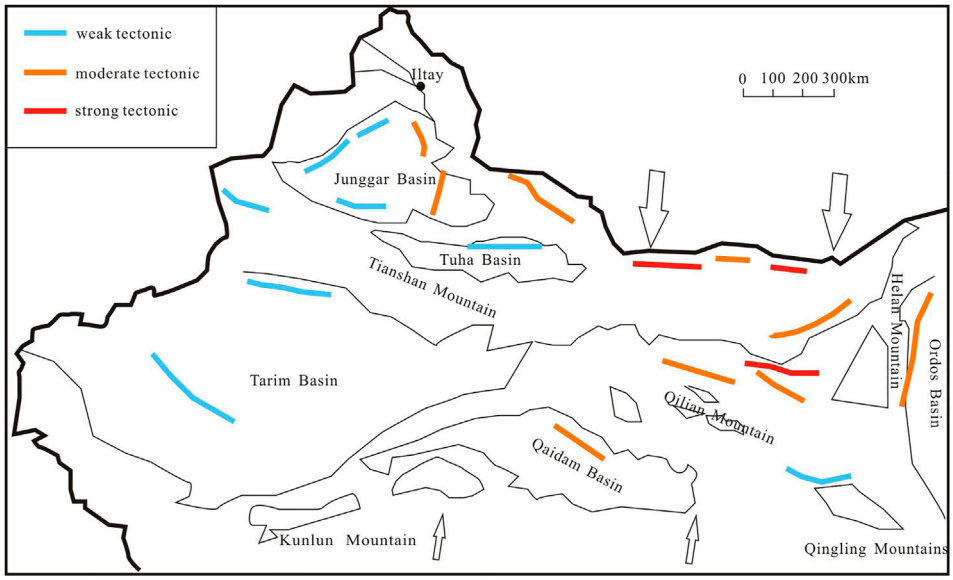

FIGURE 8
Structural strength characteristics of middle Yanshanian in Northwest China (modified from Chen et al., 2004).

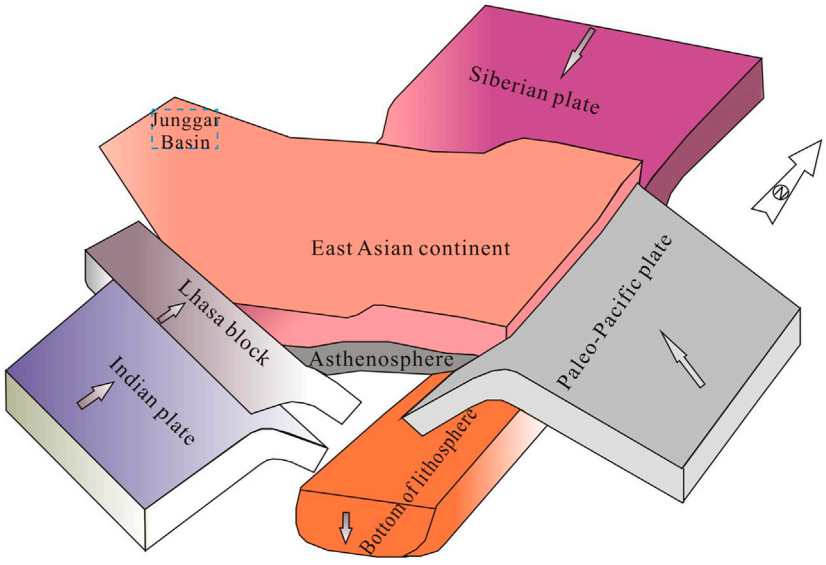

FIGURE 9
Schematic diagram of Mesozoic multi-plate convergence in East Asia continent.

Basin and its adjacent areas, which may have been the result of a distal collision between the Kohistan–Dras island arc and the Lhasa terrane.

Influence of the yanshanian orogeny on the Junggar Basin

The Yanshanian orogeny, a major geological tectonic event, occurred after the formation of the Triassic continent in East Asia. Beginning around 170 Ma in the Middle Jurassic, there were three main successive tectonic periods: a deformation period (175–136 Ma), an extension period (135–90 Ma), and a weak compression–deformation period (89–80 Ma) (Dong et al., 2019). The Yanshanian orogeny substantially influenced the tectonic evolution of eastern China; however, in northwest China, the effects of the Yanshanian orogeny seem to be relatively weak (Figure 8). A regional tectonic uplift event led to the shrinking of a sedimentary basin (Chen et al., 2004; Jia et al., 2005).

Generally, the effects of the Yanshanian orogeny on the Junggar Basin were relatively minor and mainly manifested *via* the overall

uplift of the basin, the narrowing and discontinuity of Jurassic sedimentation, and the deposition of glutenite in front of the orogenic belt (Jia et al., 2005; Zhang et al., 2006; He and Gao, 2008). Consequently, the Yanshanian orogeny in the Junggar Basin has mostly been ignored. However, widely developed unconformity at the base of Cretaceous strata is found in the Junggar Basin and across western China (Zhou and Cai, 1990; Jia et al., 2005; He and Gao, 2008; Yang et al., 2015; Yang et al., 2017) and stretches as far west as Kazakhstan (Jolivet et al., 2013). Additionally, the Yanshanian orogeny transformed Jurassic and younger strata *via* large-scale uplift and denudation, formation of a thrust system, multiple large-scale uplifts, and reactivation of large-scale faults in western China (Hendrix et al., 1992; He and Gao, 2008; Dong et al., 2019). This indicates that the Yanshanian orogeny was an important regional tectonic event.

Driving force of the yanshanian tectonic events in northwest China

With the disintegration of the united paleocontinent, three giant continental margin convergence orogenic systems (i.e., the Mongolia–Okhotsk orogenic system in the north, the Paleo-Pacific orogenic system in the east, and the Bangonghu–Nujiang orogenic system in the west) were formed around the East Asian continent in the Jurassic. Deformation and propagation of these marginal tectonic belts to the interior of the continent led to a large-scale intracontinental orogeny that formed the Yanshanian multiplate convergence tectonic system (Figure 9). The Mongolia–Okhotsk orogenic system, proximal to the northeast Junggar Basin, is a northeast-trending orogenic belt. The closing of the Mongolia–Okhotsk ocean occurred about 182–174 Ma, and the metamorphic peak of the collision zone occurred about 175–165 Ma (Zorin, 1999; Mo et al., 2005). This tectonic event may have been the driving force for the development of the Middle and Late Jurassic unconformity in the northern Junggar Basin and its adjacent areas. During the Late Jurassic–Early Cretaceous, the Lhasa block collided with the southern edge of Asia and the Bangong–Nujiang Tethys Ocean was completely closed (Allen et al., 1994; Jolivet et al., 2001), which may have exacerbated tectonic deformation in the northern Junggar Basin and its adjacent areas. Additionally, the northeast–southwest directed continental collision between the Kolyma–Omolon block in northeast Russia and the Siberian craton during the Late Jurassic to Early Cretaceous (Oxman, 2003) resulted in compressive stress transfer from the northeast edge of Siberia to Junggar and its adjacent areas through the rigid Siberian craton. In the Late Cretaceous, the Gangdise block collided with the Lhasa block (Hendrix et al., 1992). The combination of these block collisions led to an intracontinental orogeny in Central Asia and a cooling uplift event in the late Mesozoic. The opening and development of the Yanshanian tectonic events were closely related to the plate convergence and collision of the Paleo-Pacific, Tethys, and Mongolia–Okhotsk tectonic domains. The tectonic evolution of the Junggar Basin and its adjacent areas has been affected by these multiplate compression and collision events.

Conclusion

1) The central AFT and ZFT ages in the northern Junggar Basin are 131–42 Ma and 205–132 Ma, respectively.
2) These new thermochronological data indicate that the tectonic evolution of the northern Junggar Basin mainly occurred in 165–161, 93–81, and 72–66 Ma. We have interpreted the 165–161 Ma tectonic thermal event as the result of magmatism and the 93–81 and 72–66 Ma events as uplift and cooling events, respectively. We prove that the magmatism indicates the opening of the Yanshanian orogeny in the Junggar Basin, and the 93–86 and 72–64 Ma uplift and cooling events are the results of the collision between the Kohistan–Dras island arc and the Lhasa terrane.
3) Our new FT data thermochronologically confirm the Yanshanian tectonic evolution in the northern Junggar Basin, which confirms that the Yanshanian orogeny, a regional tectonic event, may have extended to northwest China.

Data availability statement

The datasets presented in this study can be found in online repositories. The names of the repository/repositories and accession number(s) can be found in the article/supplementary material.

Author contributions

ZL was responsible for the methodology and writing of this paper. ZC, YF, XL, and LY conducted the field work and collected the samples. SZ was responsible for language checking, grammar proofreading, and editing.

Funding

This study was funded by the National Natural Science Foundation of China (No. 42162015) and the Youth Science and Technology Foundation of Gansu Province (No. 20JR10RA139).

Conflict of interest

The authors declare that the research was conducted in the absence of any commercial or financial relationships that could be construed as a potential conflict of interest.

Publisher's note

References

Allen, M. B., Windley, B. F., and Zhang, C. C. (1994). Cenozoic tectonics in the urumqi-korla region of the Chinese tien Shan. *Geol. Chau* 83, 406–416. doi:10.1007/bf00210554

Ansberque, C., Godard, V., Olivetti, V., Bellier, O., de Sigoyer, J., Bernet, M., et al. (2018). Differential exhumation across the longriba fault system: Implications for the eastern Tibetan plateau. *Tectonics* 37, 663–679. doi:10.1002/2017tc004816

Bernet, M. A. (2009). A field-based estimate of the zircon fission-track closure temperature. *Chem. Geol.* 259, 181–189. doi:10.1016/j.chemgeo.2008.10.043

Bernet, M. (2019). Exhumation studies of mountain belts based on detrital fission track analysis on sand and sandstones. *Fission-Track Thermochronology its Appl. Geol.*, 269–277.

Bernet, M., and Garver, J. I. (2005). Fission track analysis of detrital zircon. *Rev. Mineralogy Geochem.* 58, 205–237. doi:10.2138/rmg.2005.58.8

Brandon, M. T. (2002). Decomposition of mixed grain age distributions using binomfit. *Track* 24, 13–18.

Brandon, M. T. (1996). Probability density plot for fission-track grain-age samplesfission-track grain-age samples. *Radiat. Meas.* 26, 663–676. doi:10.1016/s1350-4487(97)82880-6

Braun, J., Beek, P. D., and Batt, G. (2006). *Quantitative thermochronology: Numerical methods for the interpretation of thermochronological data*. Cambridge: Cambridge University Press.

Cai, Z. X., Chen, F. J., and Jia, Z. Y. (2000). Types and tectonic evolution of Junggar Basin. *Geosci. Front.* 7, 431–440.

Cao, Y., Chen, F., and Zhao, F. (2020). Tectono-magmatic events in Junggar Basin during jurassic period. *Geol. Xinjiang* 38, 341–347.

Chen, F. J., Zhang, G. Y., and Chen, Z. N. (2004). Fe/Zn double metal cyanide (DMC) catalyzed ring-opening polymerization of propylene oxide. *Geoscience* 18, 269–272. doi:10.1016/j.porgcoat.2004.03.003

Chen, F. W., Li, H. Q., Gong, D. H., Cai, H., and Chen, W. (1999). New evidence from isotopic geochronology of Yanshanian diagenesis and mineralization in the Altay orogenic belt, China. *Chin. Sci. Bull.* 44, 1142–1148.

Dodson, M. H. (1973). Closure temperature in cooling geochronological and petrologicalsystems. *Contributions Mineralogy Petrology* 40, 259–274. doi:10.1007/bf00373790

Dong, S. W., Wu, X. H., Wu, Z. H., Deng, J. F., Gao, R., and Wang, C. S. (2000). On tectonic seesawing of the East Asia continent-Global implication of the Yanshan movement. *Geol. Rev.* 46, 8–13.

Dong, S. W., Zhang, Y. Q., Li, H. L., Shi, W., Xue, H. M., Li, J. H., et al. (2019). The yanshan orogeny and late mesozoic multi-plate convergence in East asia—commemorating 90th years of the "yanshan orogeny. *Sci. China Earth Sci.* 61, 1888–1909. doi:10.1007/s11430-017-9297-y

Dong, S. W., Zhang, Y. Q., Long, C. X., Yang, Z. Y., Ji, Q., Wang, T., et al. (2007). Jurassic tectonic revolution in China and New interpretation of the Yanshanian movement. *Acta Geol. Sin.* 81, 1449–1461.

Dong, S. W., Zhang, Y. Q., Zhang, F. Q., Cui, J. J., Chen, X. H., Zhang, S. H., et al. (2015). LateJurassic-early cretaceous continental convergence and intracontinental orogenesis in East Asia: A synthesis of the yanshan revolution. *Asian Earth Sci.* 114, 750–770. doi:10.1016/j.jseaes.2015.08.011

Fang, S. H., Song, Y., and Jia, C. Z. (2006). Relationship between Cretaceous basal conglomerate and oil/gas reservoiring in the Junggar Basin. *Nat. Gas. Ind.* 26, 13–16.

Fang, Y. N., Wu, C. D., Guo, Z. J., Hou, K. J., Dong, L., Wang, L. X., et al. (2015). Provenance of the southern Junggar Basin in the Jurassic: Evidence from detrital zircon geochronology and depositional environments. *Sediment. Geol.* 315, 47–63. doi:10.1016/j.sedgeo.2014.10.014

Faure, M., Lin, W., and Chen, Y. (2012). Is the Jurassic (Yanshanian) intraplate tectonics of North China due to westward indentation of the North China block? *Terra nova.* 24, 456–466. doi:10.1111/ter.12002

Galbraith, R. F., and Green, P. F. (1990). Estimating the component ages in a finite mixturefinite mixture. *Nucl. Tracks Radiat. Meas.* 17, 197–206. doi:10.1016/1359-0189(90)90035-v

Galbraith, R. F., and Laslett, G. M. (1997). Statistical modelling of thermal annealing of fission tracks in zirconfission tracks in zircon. *Chem. Geol.* 140, 123–135. doi:10.1016/s0009-2541(97)00016-8

Galbraith, R. F., and Laslett, G. M. (1993). Statistical models for mixed fission track agesfission track ages. *Nucl. Tracks Radiat. Meas.* 21, 459–470. doi:10.1016/1359-0189(93)90185-c

Gallagher, K., Brown, R. W., and Johnson, C. (1998). Fission track analysis and its applications to geological problems. *Annu. Rev. Earth Planet. Sci.* 26, 519–572. doi:10.1146/annurev.earth.26.1.519

Ge, X., Shen, C., Selby, D., Deng, D., and Mei, L. (2016). Apatite fission-track and Re-Os geochronology of the xuefeng uplift, China: Temporal implications for dry gas associated hydrocarbon systemsfission-track and Re-osgeochronology of the xuefeng uplift, China: Temporal implications for dry gas associated hydrocarbon systems. *Geology* 44, 491–494. doi:10.1130/g37666.1

Gleadow, A. J. W., Duddy, I. R., Green, P. F., and Lovering, J. F. (1986). Confined fission track lengths in apatite: A diagnostic tool for thermal history analysis. *Contributions Mineralogy Petrology* 94, 405–415. doi:10.1007/bf00376334

Glorie, S., Grave, J. D., Buslov, M. M., Elburg, M. A., Stockli, D. F., Gerdes, A., et al. (2010). Multi-method chronometric constraints on the evolution of the northern Kyrgyz tien Shan granitoids (central asian orogenic belt): From emplacement to exhumation. *J. Asian Earth Sci.* 38, 131–146. doi:10.1016/j.jseaes.2009.12.009

Green, P. F. (1985). Comparison of zeta calibration baselines for fission-track dating of apatite, zircon and sphenefission-track dating of apatite, zircon and sphene. *Chem. Geol.* 58, 1–22. doi:10.1016/0168-9622(85)90023-5

Guo, Z. J., Zhang, Z. C., and Liao, G. H. (2002). Uplifting process of eastern Tianshan mountains: Evidence from fission track age and its tectonic significance. *Xinjiang Geol.* 20, 331–334.

Guo, Z. J., Zhang, Z. C., Wu, C. D., Fang, S. H., and Zhang, R. (2006). The mesozoic and cenozoic exhumation history of tianshan and comparative studies to the junggar and Altai mountains. *Acta Geol. Sin.* 80, 1–15.

Han, B. F., Ji, J. Q., Sun, B., Chen, L. H., and Zhang, L. (2006). Late Paleozoic vertical growth of continental crust around the Junggar Basin, Xinjiang, China (part1): Timing of post-collisional plutonism. *Acta Petrol. Sin.* 22, 1077–1086.

He, Z. L., and Gao, S. L. (2008). The Yanshanian movement and its control over hydrocarbon accumulation in Western China. *Oil Gas Geol.* 29, 419–427.

He, Z. Y., Wang, B., Glorie, S., Su, W. B., Ni, X. H., Jepson, G., et al. (2022b). Mesozoic building of the eastern tianshan and east Junggar (NW China) revealed by low-temperature thermochronology. *Gondwana Res.* 103, 37–53. doi:10.1016/j.gr.2021.11.013

He, Z. Y., Wang, B., Nachtergaele, S., Glorie, S., Ni, X. H., Su, W. B., et al. (2021). Long-term topographic evolution of the Central Tianshan (NW China) constrained by low-temperature thermochronology. *Tectonophysics* 817, 229066. doi:10.1016/j.tecto.2021.229066

He, Z. Y., Wang, B., Su, W. B., Glorie, S., Ni, X. H., Liu, J. S., et al. (2022a). Meso-Cenozoic thermo-tectonic evolution of the Yili block within the Central Asian Orogenic Belt (NW China): Insights from apatite fission track thermochronology. *Tectonophysics* 823, 229194. doi:10.1016/j.tecto.2021.229194

Hendrix, M. S., Dumitru, T. A., and Graham, S. A. (1994). Late oligocene early miocene unroofing in the Chinese tianshan: An early effect of the India-Asia collision. *Geology* 22, 487–490. doi:10.1130/0091-7613(1994)022<0487:loemui>2.3.co;2

Hendrix, M. S., Graham, S. A., Carroll, A. R., Sobel, E. R., Mcknight, C. L., Schulein, B. J., et al. (1992). Sedimentary record and climatic implications of recurrent deformation in the Tian Shan: Evidence from Mesozoic strata of the north Tarim, south Junggar, and Turpan basins, northwest China. *Geol. Soc. Am. Bull.* 104, 53–79. doi:10.1130/0016-7606(1992)104<0053:sracio>2.3.co;2

Hou, G. F., Zeng, D. L., and Niu, Z. J. (2020). New discovery of sandy debris flow sandbody and its implications foroil and gas exploration in the Junggar Basin. *Nat. Gas. Ind.* 40, 41–49.

Hurford, A. J., and Green, P. F. (1983). The zeta age calibration of fission track dating. *Chem. Geol.* 41, 285–317. doi:10.1016/s0009-2541(83)80026-6

Hurford, A. J. (1991). Uplift and cooling pathways derived from fission track analysis and mica dating: A review. *Geol. Rundsch.* 80, 349–368. doi:10.1007/bf01829371

Jia, C. Z., Wei, G. Q., and Li, B. L. (2005). Yanshanian tectonic features in West-central China and their petroleum geological significance. *Oil Gas Geol.* 26, 9–15.

Jian, X., Guan, P., Zhang, W., Liang, H., Feng, F., and Fu, L. (2018). Late cretaceous to early eocene deformation in the northern Tibetan plateau: Detrital apatite fission track evidence from northern qaidam basin. *Gondwana Res.* 60, 94–104. doi:10.1016/j.gr.2018.04.007

Johan, D. G., Michael, M. B., and Peter, V. H. (2006). Distant effect s of India Eurasia convergence and Mesozoic intracontinental deformation in Central Asia: Constraints from apatite fission-track thermo-chronology. *J. Asian Earth Sci.* 3, 1–17.

Jolivet, M., Brunel, M., Seward, D., Xu, Z., Yang, J., Roger, F., et al. (2001). Mesozoic and cenozoic tectonics of the northern edge of the Tibetan plateau: Fission-track constraints. *Tectonophysics* 343, 111–134. doi:10.1016/s0040-1951(01)00196-2

Jolivet, M., Heilbronn, G., Robin, C., Barrier, L., Bourquin, S., Guo, Z., et al. (2013). Reconstructing the Late Palaeozoic-Mesozoic topographic evolution of the Chinese Tianshan: Available data and remaining uncertainties. *Adv. Geosciences* 37, 7–18. doi:10.5194/adgeo-37-7-2013

Ketcham, R. A. (2005). Forward and inverse modeling of low-temperature thermochronometry data. *Rev. Mineralogy Geochem.* 58, 275–314. doi:10.2138/rmg.2005.58.11

Ketcham, R. A., vander, B. P., Barbarand, J., Bernet, M., and Gautheron, C. (2018). Reproducibility of thermal history reconstruction from apatite fission-track and (U-Th)/He datafission-track and (U-Th)/He data. *Geochem. Geophys. Geosystems* 19, 2411–2436. doi:10.1029/2018gc007555

Laslett, G. M., Green, P. F., Duddy, I. R., and Gleadow, A. J. W. (1987). Thermal annealing of fission tracks in apatite: A quantitative analysis. *Chem. Geology:Isotope Geosci. Sect.* 65, 1–13. doi:10.1016/0168-9622(87)90057-1

Li, W., Hu, J. M., and Qu, H. J. (2010). Fission track analysis of Junggar Basin peripheral orogenand its geological significance. *Acta Geol. Sin.* 84, 171–182.

Li, Z. H., Chen, G., Cui, J. B., Chen, Z. J., H, J. Y., Ding, C., et al. (2014). Fission track age of yanshanian tectonic-thermal events in the northern Junggar Basin. *Geol. Sci. Technol. Inf.* 33, 9–14.

Liu, S. B., Dou, H., Li, H. B., and Wen, Z. G. (2019). Geological significance of the discovery of Late Jurassic intermediate-acidic intrusive rock in Bogeda area of East Tianshan, Xinjiang, and its U-Pb zircon age. *Geol. Bull. China* 38, 288–294.

Liu, S. B., Dou, H., Zhang, W. M., Peng, Z. J., Zhang, L., and Zhang, W. R. (2018). Discovery of Jurassic trachyandesite and its geological significance in the northwestern of Junggar Basin. *Geol. Rev.* 64, 1519–1529.

Luo, M., Zhu, W. B., Zheng, B. H., and Zhu, X. Q. (2012). Mesozoic-Cenozoic tectonic evolution of the Kuqa Basin: Evidence from apatite fission track data. *Earth Sci.* 37, 893–902.

Mo, S. G., Han, M. L., and Li, J. Z. (2005). Composition and orogeny of Mongolia Okhotsk orogenic belt Process. *J. Shandong Univ. Sci. Technol.* 24, 50–52.

Oxman, V. S. (2003). Tectonic evolution of the mesozoic verkhoyansk-kolyma belt (NE Asia). *Tectonophysics* 365, 45–76. doi:10.1016/s0040-1951(03)00064-7

Patel, R. C., Singh, P., and Lal, N. (2015). Thrusting and back-thrusting as post-emplacement kinematics of the AlmoraKlippe: Insights from low-temperature thermochronology. *Tectonophys* 653, 41–51. doi:10.1016/j.tecto.2015.03.025

Patel, R. C., Sinha, H. N., Kumar, B. A., and Singh, P. (2014). Basin provenance and post-depositional thermal history along the continental P/T boundary of the Raniganj basin, eastern India: Constraints from apatite fission track datingfission track dating. *J. Geol. Soc. India.* 83, 403–413. doi:10.1007/s12594-014-0057-7

Qiu, L., Kong, R. Y., Yan, D. P., Mu, H. X., Sun, W. H., Sun, S., et al. (2022a). Paleo–Pacific plate subduction on the eastern Asian margin: Insights from the Jurassic foreland system of the overriding plate. *GSA Bull.* 134, 2305–2320. doi:10.1130/b36118.1

Qiu, L., Kong, R. Y., Yan, D. P., Wells, M. L., Wang, A., Sun, W., et al. (2018). The Zhayao tectonic window of the Jurassic Yuantai thrust system in Liaodong Peninsula, NE China: Geometry, kinematics and tectonic implications. *J. Asian Earth Sci.* 06, 58–71. doi:10.1016/j.jseaes.2018.06.012

Qiu, L., Yan, D. P., Ma, H. B., Sun, S. H., Deng, H. L., Zhou, Z. C., et al. (2022b). Late Cretaceous geodynamics of the Palaeo-Pacific plate inferred from basin inversion structures in the Songliao Basin (NE China). *Terra nova.* 34, 465–473. doi:10.1111/ter.12612

Qiu, N. S., Yang, H. B., and Wang, X. L. (2002). Tectonic thermal evolution of Junggar Basin. *Geol. Sci.* 37, 423–429.

Ruiz, G. M. H., Seward, D., and Winkler, W. (2004). Detrital thermochronology-a new perspective on hinterland tectonics, an example from the Andean Amazon Basin, Ecuador. *Basin Res.* 16, 413–430. doi:10.1111/j.1365-2117.2004.00239.x

Sun, W. J., Zhao, S. J., Li, S. Z., and Li, T. (2018). Mesozoic tectonic migration in eastern Junggar Basin. *Geotect. Metallogenia* 38, 52–61.

Tian, P. F., Yuan, W. M., and Yang, X. Y. (2020a). Basic principles, important concepts and geological applications of thermochronology. *Geol. Rev.* 66, 975–1003.

Tian, P. F., Yuan, W. M., Yang, X. Y., Feng, Z. R., Chen, X., and Yuan, E. J. (2020b). Multi-stage tectonic events of the Eastern Kunlun Mountains, Northern Tibetan Plateau constrained by fission track thermochronology. *J. Asian Earth Sci.* 198, 104428. doi:10.1016/j.jseaes.2020.104428

Wang, J. B., and Xu, X. (2006). Post collisional tectonic evolution and mineralization in Northern Xinjiang. *Acta Geol. Sin.* 80, 23–31.

Wu, Z. J., Han, X. Z., Ji, H., Cai, Y. F., Xue, L., and Sun, S. J. (2021). Mesozoic-Cenozoic tectonic events of eastern Junggar Basin, NW China and their significance for uranium mineralization: Insights from seismic profiling and AFT dating analysis. *Ore Geol. Rev.* 139, 104488. doi:10.1016/j.oregeorev.2021.104488

Xiao, W. J., Song, D. F., Windley, B. F., Li, J. L., Han, C. M., Wan, B., et al. (2020). Accretionary processes and metallogenesis of the Central Asian Orogenic Belt: Advances and perspectives. *Sci. China Earth Sci.* 63 (3), 33.

Xiao, X. C., Tang, Y. Q., and Feng, Y. M. (1992). *Geotectonics of northern Xinjiang and its adjacent areas.* Beijing: Geology Press, 16–42.

Yan, D. P., and Qiu, L. (2020). Geology of China and adjacent regions: An introduction. *J. Asian Earth Sci.* 203, 104533. doi:10.1016/j.jseaes.2020.104533

Yang, P., Wu, G. H., Ren, Z. L., Zhou, R. J., Zhao, J. X., and Zhang, L. P. (2020). Tectono-thermal evolution of Cambrian–Ordovician source rocks and implications for hydrocarbon generation in the eastern Tarim Basin, NW China. *J. Asian Earth Sci.* 194, 104267. doi:10.1016/j.jseaes.2020.104267

Yang, W., Jolivet, M., Guo, Z. J., Zhang, Z. C., and Wu, C. D. (2013). Source to sink relations between the tianshan and Junggar Basin (northwest China) from late palaeozoic to quaternary: Evidence from detrital U-Pb zircon geochronology. *Basin Res.* 22, 219–240. doi:10.1111/j.1365-2117.2012.00558.x

Yang, Y. T., Guo, Z. X., and Luo, Y. J. (2017). Middle-late jurassic tectonostratigraphic evolution of central Asia, implications for the collision of the karakoram-lhasa block with Asia. *Earth Sci. Rev.* 166, 83–110. doi:10.1016/j.earscirev.2017.01.005

Yang, Y. T., Song, C. C., and He, S. (2015). Jurassic tectonostratigraphic evolution of the Junggar Basin, NW China: A record of mesozoic intraplate deformation in central Asia. *Tectonics* 34, 86–115. doi:10.1002/2014tc003640

Yuan, W. M., Dong, J. Q., Tang, Y. H., and Bao, Z. K. (2004). Thermal history of the Tiereketi batholith in Altay Mountains, northern Xinjiang: Evidence from apatite fission track analysis. *Acta Geosci. Sin.* 25, 199–204.

Zattin, M., and Wang, X. X. (2019). Exhumation of the Western Qinling mountain range and the building of the northeastern margin of the Tibetan Plateau. *J. Asian Earth Sci.* 177, 307–313. doi:10.1016/j.jseaes.2019.04.002

Zaun, P. E., and Wagner, G. A. (1985). Fission-track stability in zircons under geological conditions. *Nucl. Tracks Radiat. Meas.* 10, 303–307. doi:10.1016/0735-245x(85)90119-x

Zhang, C. J., He, D. F., and Shi, X. (2006). Formation and evolution of multi-cycle superimposed Basin in junggar. *Pet. Geol.* 1, 47–58.

Zhang, H. H., Zhang, Z. C., Tang, W. H., Li, K., Li, J. F., Wang, Q., et al. (2022). Burial and exhumation history of Jurassic sedimentary rocks in the southern margin of the Junggar BasinImplications for the growth of the northern Tianshan Mountains. *J. Asian Earth Sci.* 236, 105339.

Zhang, Q. F., Hu, A. Q., and Zhang, G. X. (1994). Isotopic age evidence of Mesozoic Cenozoic magmatism in Altay area. *Geochemistry* 23, 269–280.

Zhang, W. G., Chen, Z. L., and Cai, L, B. (2017). Fission track evidence of Cretaceous uplift exhumation in Western Tianshan. *Acta Geol. Sin.* 91, 510–522.

Zhao, B. (1992). Formation and evolution of Junggar Basin. *Petroleum Geol. Xinjiang* 13, 191–196.

Zhou, L. R., and Cai, H. W. (1990). Yanshan movement in Northwest China northwest geosciences. *Northwest Geosci.* 30, 64–78.

Zhu, W. B., Wan, J. L., and Shu, L. S. (2005). Application of fission track technology in structural evolution. *Acta Geol. Sin. Sin.* 11, 593–600.

Zhu, W. B., Wang, F. J., Cao, Y. Y., and Wang, S. L. (2020). Tectono-magmatic events in tianshan mountains and adjacent areas during yanshanian movement period. *Acta Geol. Sin.* 94, 1331–1346.

Zorin, Y. A. (1999). Geodynamics of the Western part of the Mongolia-Okhotsk collisional belt, trans-Baikal region (Russia) and Mongolia. *Tectonophysics* 306, 33–56. doi:10.1016/s0040-1951(99)00042-6